Solar Irradiance Variability Due to Solar Flares Observed in Lyman-Alpha Emission

Ryan O. Milligan[1]

Abstract As the Lyman-alpha (Lyα) line of neutral hydrogen is the brightest emission line in the solar spectrum, detecting increases in irradiance due to solar flares at this wavelength can be challenging due to the very high background. Previous studies that have focused on the largest flares have shown that even these extreme cases generate enhancements in Lyα of only a few percent above the background. In this study, a superposed-epoch analysis was performed on $\approx$8500 flares greater than B1 class to determine the contribution that they make to changes in the solar EUV irradiance. Using the peak of the $1-8$ Å X-ray emission as a fiducial time, the corresponding time series of 3123 B- and 4972 C-class flares observed in Lyα emission by the EUV Sensor on the Geostationary Operational Environmental Satellite 15 (GOES-15) were averaged to reduce background fluctuations and improve the flare signal. The summation of these weaker events showed that they produced a $0.1-0.3\%$ enhancement to the solar Lyα irradiance on average. For comparison, the same technique was applied to 453 M- and 31 X-class flares, which resulted in a $1-4\%$ increase in Lyα emission. Flares were also averaged with respect to their heliographic angle to investigate any potential center-to-limb variation. For each GOES class, the relative enhancement in Lyα at the flare peak was found to diminish for flares that occurred closer to the solar limb due to the opacity of the line and/or foreshortening of the footpoints. One modest event included in the study, a C6.6 flare, exhibited an unusually high increase in Lyα of 7% that may have been attributed to a failed filament eruption. Increases of this magnitude have hitherto only been associated with a small number of X-class flares.

Keywords Solar flares · Solar chromosphere · Lyman-alpha · Solar Irradiance · Center-to-limb variation

✉ R.O. Milligan
r.milligan@qub.ac.uk

[1] Astrophysics Research Centre, School of Mathematics and Physics, Queen's University Belfast, University Road, Belfast, BT7 1NN, Northern Ireland, UK

1. Introduction

The Lyman-alpha (Lyα) line of neutral hydrogen at 1216 Å is the brightest emission line in the solar spectrum. It results from the 2p–1s transition, and in the quiet-Sun, its formation height ranges from the mid-chromosphere (≈6,000 K; line wings) to the base of the transition region (≈40,000 K; line core). During solar flares, nonthermal electrons deposit their energy at these layers, generating localised heating and ionization at the flare footpoints. Precisely how the Lyα line responds to this injection of energy remains unknown due to the lack of spectrally-resolved measurements of this fundamental line during flares. One exception is a serendipitous observation of the 28 October 2003 X17 flare by Woods et al. (2004). They found that the line core increased by around 20% while the line wings were enhanced by around factor of two, with the blue wing responding more than the red wing (see also Canfield and van Hoosier, 1980; Brekke et al., 1996; and Milligan and Chamberlin, 2016). However, even in this case the data were recorded with a scanning spectrograph and so different parts of the line profile may have been sampled at different stages of the flare's impulsive phase.

Lyα is believed to be a significant radiator of flare energy, accounting for several percent of the total radiated energy in a single emission line (Rubio da Costa et al., 2009; Milligan et al., 2014). It has also recently been shown that flare-induced acoustic oscillations can be detected in disc-integrated Lyα observations, suggesting a potential diagnostic for the dissipation of mechanical energy as well (Milligan et al., 2017, 2020). The study of flares in Lyα is also crucial for the field of space weather as photons at this wavelength can induce chemical and dynamic changes in planetary atmospheres (Chubb et al., 1957; Lean, 1985; Woods et al., 1995). During quiescent solar conditions, Lyα photons get absorbed in the D-layer of Earth's ionosphere, along with solar X-rays, although Raulin et al. (2013) were unable to detect any appreciable D-layer effects during seven small-to-moderate flares observed in Lyα; these flares were found to produce Lyα enhancements < 1%. However, during an X-class flare that exhibited a ≈30% Lyα enhancement, Milligan et al. (2020) noted that the impulsive increase in Lyα emission correlated with induced currents in the E-layer due to the ionization of nitric oxide as determined from magnetometer data. The corresponding D-layer response occurred several minutes later in line with the more gradually varying soft X-rays (SXR). Further study of flares in Lyα emission and the corresponding response of the terrestrial atmosphere is required to establish if that was an isolated case, or a more common occurrence.

The few reports of solar flare observations in Lyα that previously existed were mostly from broadband, disc-integrated irradiance measurements, and often focused on small numbers of events due to the limited duty cycles of instruments capable of observing flares at this wavelength (Kretzschmar, Dominique, and Dammasch, 2013; Raulin et al., 2013; Milligan et al., 2014; Kretzschmar, 2015; Milligan and Chamberlin, 2016; Dominique et al., 2018). However, Milligan et al. (2020) recently carried out a statistical study of 477 M- and X-class flares in broadband, disc-integrated Lyα emission, and calculated the distribution of contrasts. It was found that most flares–(95%) produced less than a 10% enhancement above background, with a maximum of ≈30%, although X-class flares that occurred closer to the solar limb were found to produce less of an enhancement. They also measured how the total energy radiated in Lyα scaled with the energy radiated in X-rays; the excess solar irradiance in Lyα was found to be up to two orders of magnitude more energetic than that of the corresponding X-rays.

The study of Milligan et al. (2020) focused on larger flares as smaller GOES class events (B- and C-class) did not produce an appreciable response in Lyα above the intense background. This may be due to instrumental sensitivity, or perhaps Lyα emission from weaker

events is not inherently significant. The aim of this article is therefore to use a superposed-epoch analysis technique to determine how much of an enhancement these smaller flares would produce, if any, and how much this increase contributes to the solar irradiance at this wavelength. Kretzschmar et al. (2010) used this simple technique to determine the effects of solar flares on the total solar irradiance (TSI; solar flux over all wavelengths incident at the top of Earth's atmosphere). Using the time of peak soft X-ray emission (i.e. the $1-8$ Å channel) from the X-Ray Sensor (XRS) on board the Geostationary Operational Environmental Satellite (GOES; Hanser and Sellers, 1996) as a key time marker for several hundred flares, the corresponding TSI time series around each flare could then be coadded (or averaged) to reduce the background fluctuations (due to acoustic oscillations and granulation), thereby increasing the coherent flare signal. Similarly, Kretzschmar (2011) followed this study by using the same technique on visible, EUV, and SXR irradiance datasets from the Solar and Heliospheric Observatory (SOHO) to show that all flares can be considered to be white light flares, and that the visible component of flare emission (corresponding to a temperature of 9,000 K) can amount to 70% of the total radiated energy. Section 2 of this article describes the dataset that was used and how the analysis technique was applied. The results are presented in Section 3, while a summary and discussion are given in Section 4.

2. Data Analysis

The Extreme Ultra-Violet Sensor (EUVS; Viereck et al., 2007) on board the GOES-N series of satellites (GOES-13, GOES-14, and GOES-15) comprises five channels, A, B, C, D, and E, covering the 50–170 Å, 240–340 Å, 200–620 Å, 200–800 Å, and 1180–1250 Å wavelength ranges, respectively, with the E-channel centered on the Lyα line at 1216 Å. Each broadband channel samples the solar EUV irradiance at 10.24 s cadence, compared to the more familiar GOES-N/XRS which samples the 0.5–4 Å and $1-8$ Å wavelength ranges at 2 s cadence. While the availability of EUVS data from GOES-13 and GOES-14 has been inconsistent since their launches, GOES-15 has provided continuous coverage since its launch in 2010. However, only data taken up until 6 June 2016 have been made publicly available at the time of writing. EUVS-E data are scaled to a *Whole Heliosphere Interval* quiet-Sun reference spectrum[1] (Woods et al., 2009), providing Lyα irradiance measurements in physical units of W m^{-2}. Thus the data may not necessarily reflect flare-related time variations of the line profile, generating some systematic uncertainties. To correct for detector degradation, the EUVS-E data are scaled to the daily-averaged data from the Solar–Stellar Irradiance Comparison Experiment (SOLSTICE; McClintock, Rottman, and Woods, 2005) on board the Solar Radiation and Climate Experiment (SORCE), and only Version 4 of the EUVS-E data were used in this study.[2]

Figure 1 shows a 72-hour period from February 2011, during which, flares of a range of X-ray magnitudes occurred (top panel; the vertical dotted lines in both panels denote the peak times of each X-ray event). However, over the same period, only the largest of these events produced a discernible response in Lyα emission (bottom panel). Also visible in the bottom panel are the daily dips in detected Lyα emission due to attenuation by the Earth's geocorona—which is opaque to Lyα photons (Meier and Prinz, 1970; Baliukin et al., 2019)—for a few hours during each GOES orbit. For every event considered in this study, a 24 hour period of Lyα emission centered on the peak X-ray time of the flare was fitted with

---

[1]http://lasp.colorado.edu/lisird/data/whi_ref_spectra.

[2]https://www.ngdc.noaa.gov/stp/satellite/goes/doc/GOES_NOP_EUV_readme.pdf.
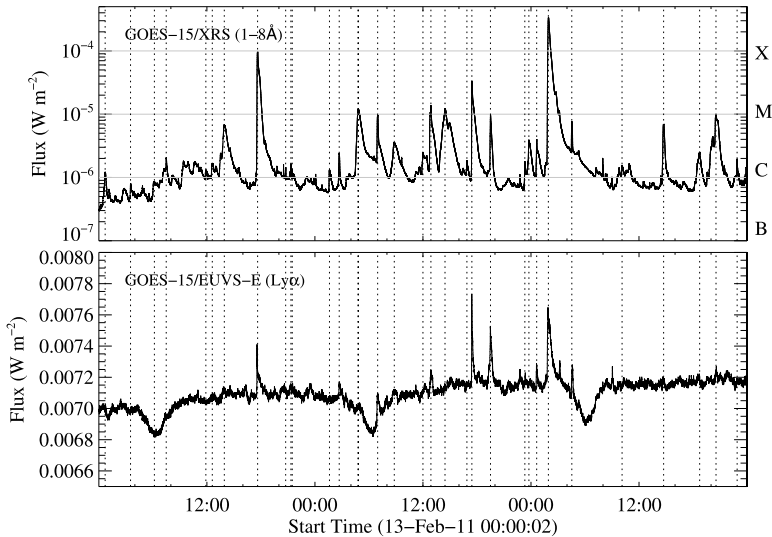
Figure 1 72 hours of X-ray (top panel) and Lyα (bottom panel) irradiance data from GOES-15 during February 2011. The vertical dotted lines in each panel denote the peak times of all events listed in the NOAA flare catalog. The daily dips in the Lyα data are due to geocoronal absorption by the Earth's outer atmosphere.

a constant, equal to the modal value, plus an inverted Gaussian (red curve in the bottom panel of Figure 2) to account for the geocoronal dip given that the amount of attenuation varies throughout the year. As the effect of the geocorona on Lyα flare irradiance is likely to be nonlinear, any events that occurred within $\pm 2\sigma$ (vertical dashed line) of the minimum of each daily dip (vertical solid line) were omitted from this study.

The start, peak, and end times of every X-ray flare are listed in the GOES event list[3] hosted by the National Oceanic and Atmospheric Administration/Space Weather Prediction Center (NOAA/SWPC). However, this list does not always include the flare location, whereas the Heliophysics Event Knowlegebase (HEK)[4] does, although it is missing several months of data throughout Solar Cycle 24 (Milligan and Ireland, 2018). The superposed-epoch technique employed in this study uses the peak time of all X-ray flares above B1 from the HEK database as a fiducial time after removing any events affected by geocoronal absorption, eclipse periods, or corrupted data. This resulted in 3123 B-class and 4972 C-class flares.[5] While the Lyα component of M- and X-class flares can often be detected above the solar background, the averaged profiles of 453 M- and 31 X-class flares were also included in this analysis. This then allows the average flux (in W m^{-2}) and contrast (relative percentage increase) to be measured for each GOES classification (Section 3). Furthermore, given the abundance of events observed by GOES-15/EUVS-E over Solar Cycle 24, and with knowledge of their locations from the HEK, the average Lyα profile can be determined as a function of heliographic angle in order to establish any potential center-to-limb variation (CLV; Section 3.1).

---

[3]https://www.ngdc.noaa.gov/stp/satellite/goes/index.html.

[4]https://www.lmsal.com/hek/.

[5]Note that there were more C-class flares than B-class flares due to the high X-ray background around the time of solar maximum.
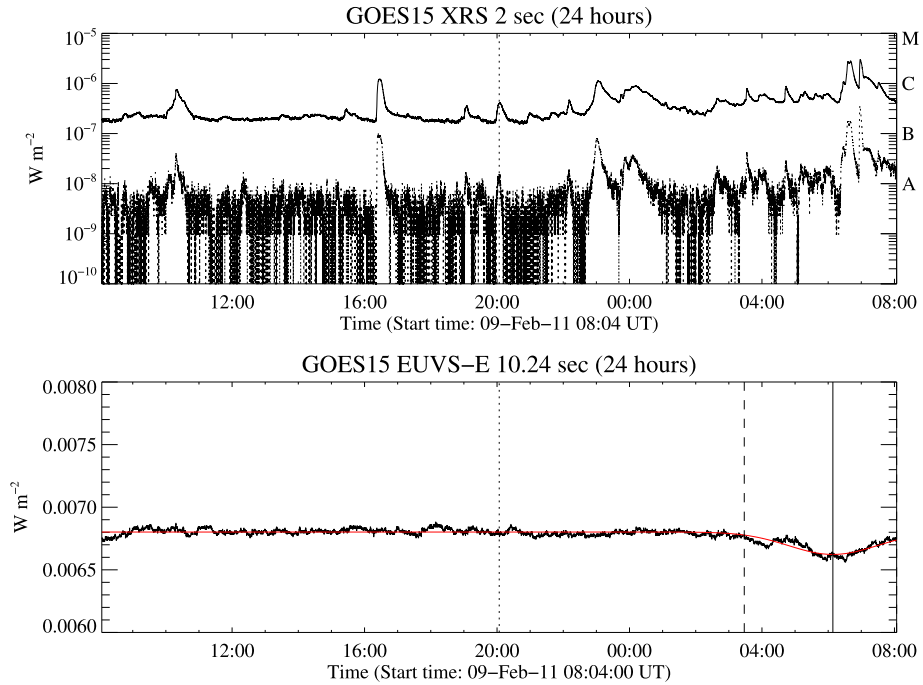
Figure 2 Top panel: 24 hours of GOES-15/XRS data at $1-8$ Å (solid curve) and $0.5-4$ Å (dotted curve) centered on the peak of the B2.9 flare that occurred on 9 February 2011 (SOL2011-02-09) beginning at 19:57 UT. The vertical dotted line denotes the peak of the B2.9 flare as listed in the NOAA event list. Bottom panel: The GOES-15/EUVS-E (Lyα) data over the same 24 hour period. The red line marks the background value over this period, taken as a constant equal to the modal value plus a Gaussian to account for geocoronal absorption, seen as a dip in the data around 06:00 UT on 10 February 2011. The vertical solid line marks the minimum of the dip, while the vertical dashed line marks the 2σ width.

A one-hour time range of the Lyα time series, from 20 minutes prior to the X-ray peak to 40 minutes after, was averaged over for all flares of a given GOES class. Four B-class flares are shown in the left hand panels of Figure 3 as an example. For each individual event, there does not appear to be any discernible Lyα enhancement due to the flare, but by averaging over increasing numbers of Lyα time series of equal length, the signal-to-noise ratio is vastly improved as shown in the right hand panel. The red, green, and blue profiles represent the summation of 10, 100, and 1000 randomly chosen B-class flares, respectively. The smoothly-varying solid black lightcurve is the result of averaging all 3123 B-class flares considered. This illustrates how the signal-to-noise ratio is increased by increasing the number of events added together.

3. Results

The four panels in Figure 4 show the average Lyα time profiles for B-, C-, M-, and X-class flares. All profiles show a clear and distinct peak in Lyα emission that was not readily visible for individual events, particularly weaker GOES classes. The average B-class flare produced an enhancement of 0.18% above background, while C-class flares showed a 0.35%
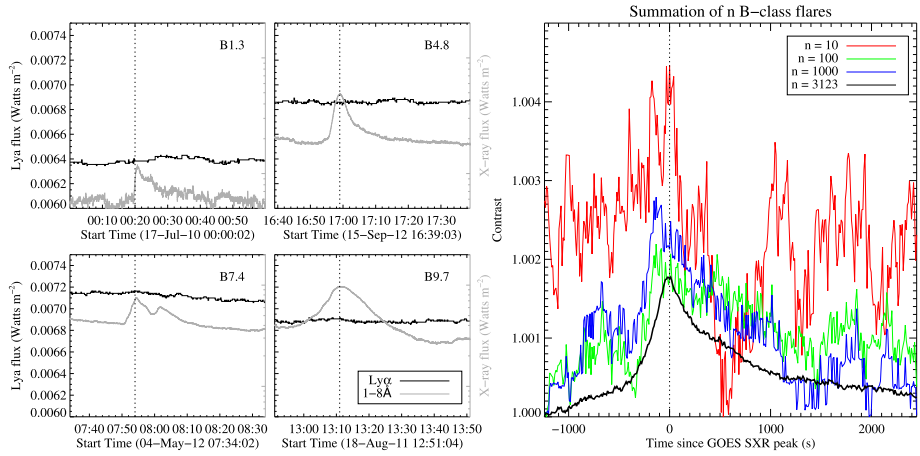
Figure 3 Left hand panels: Time profiles for four B-class flares in Lyα (black) and X-rays (gray). The scaling is the same on each panel. The vertical dotted line on each panel marks the X-ray peak as catalogued in the NOAA flare list. The right hand panel illustrates how the Lyα flare signal becomes more apparent when adding together increasing numbers of events. The red curve is the average of 10 random B-class flares, the green curve is the result of 100 events, the blue curve of 1000, and finally the black curve is an average of all 3123 B-class flares from this study.
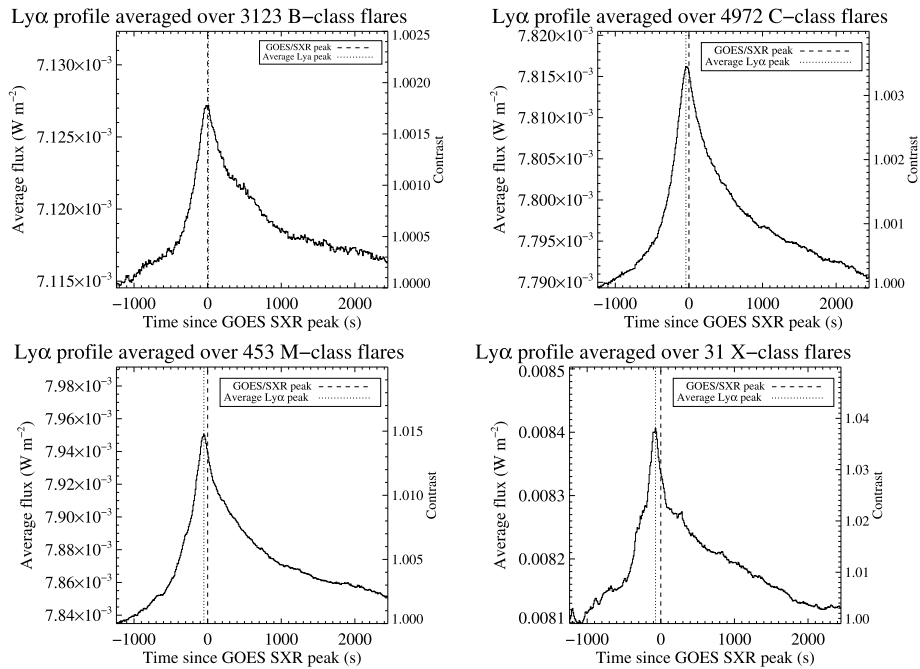
Figure 4 Plots of the average time profiles for all B-, C-, M-, and X-class flares included in this study. The vertical dashed line in each panel marks the time of the SXR peaks of all flares, while the vertical dotted line marks the peak of the Lyα emission. The contrast axis denotes the percentage increase in each panel.

increase. These values are in agreement with those reported by Raulin et al. (2013) for several C-class flares observed by Project for On-Board Autonomy 2/Large Yield Radiometer (PROBA-2/LYRA). Most individual M- and X-class flares can be readily observed in Lyα, as shown by Milligan et al. (2020), they are included here for completeness. M-class flares were measured to increase the solar irradiance by 1.5% on average, while X-class flares exhibited a 3.8% increase in Lyα above background. Although the flare-related changes in Lyα irradiance quoted here are quite small, these changes can still correspond to a significant amount of radiated energy. This confirms that weaker flares do have associated responses in Lyα emission that are ordinarily obscured by the intense solar background. This will have significant implications for more sensitive Lyα instruments that aim to observe solar flares in the future.

The peak timings of the averaged profiles are also shown in Figure 4 as vertical dotted lines. For B-class flares, the average peak time coincides with the peak of the SXR emission for the summed events to within one GOES-15/EUVS-E time bin (10.24 s). For C-class flares, Lyα peaks slightly earlier than the X-ray peak (40.96 s; four time bins), while M- and X-class flares peak even earlier still (51.20 s and 71.68 s, respectively). This somehow implies that Lyα emission from B-class flares may be thermally generated, while C-, M-, and X-class flares exhibit more nonthermal Lyα emission in accordance with the Neupert effect (Neupert, 1968). Although it is tempting to assume that this systematic change in peak timing is physically significant, great care must be taken in drawing conclusions from summed epoch analyses as individual events can sometimes skew the resulting profile.

3.1. Center-to-Limb Variation

As Lyα is optically thick (Woods et al., 2000), flares that occur closer to the solar limb are assumed to produce less of a response in Lyα than if they had occurred at disc center due to scattering by the increasing column mass along the line-of-sight. Milligan et al. (2020) showed that this was true for 31 X-class flares by normalising their Lyα flux to their X-ray flux (which is optically thin) and showing that this ratio decreases with increasing heliocentric angle from disc center. This center-to-limb variation was also confirmed through a stereoscopic observation of an X-class limb event as viewed by GOES-15 from Earth that was observed simultaneously by the EUV Monitor on board the Mars Atmospheric and Volatile Evolution satellite (MAVEN/EUM; Eparvier et al., 2015), when Earth and Mars were around 90 degrees apart. After correcting for the Earth-Mars distance and light travel time, the flux detected by MAVEN (which observed the flare close to disc center) was greater than that detected by GOES.

Figure 5 shows averaged flare time profiles for the four GOES classes in increments of 10 degrees from 0–90°. In most cases, flares that occurred closer to disc center had a higher absolute flux value, and a more pronounced peak relative to the background around the time of the GOES SXR peak. This trend breaks down for X-class flares due to the diminishing number of events. To illustrate this point, Figure 6 shows the contrast value (peak flux divided by minimum flux) for each heliographic angle bin for B-, C-, and M-class flares. Error bars were taken as the 1σ value for each curve in Figure 5 divided by the square root of the number events in each bin (Kretzschmar et al., 2010). These data points were fitted with the commonly used CLV function:

$$R = R_C \left(k + 2(1-k) \left(\mu - \frac{\mu^2}{2} \right) \right), \tag{1}$$
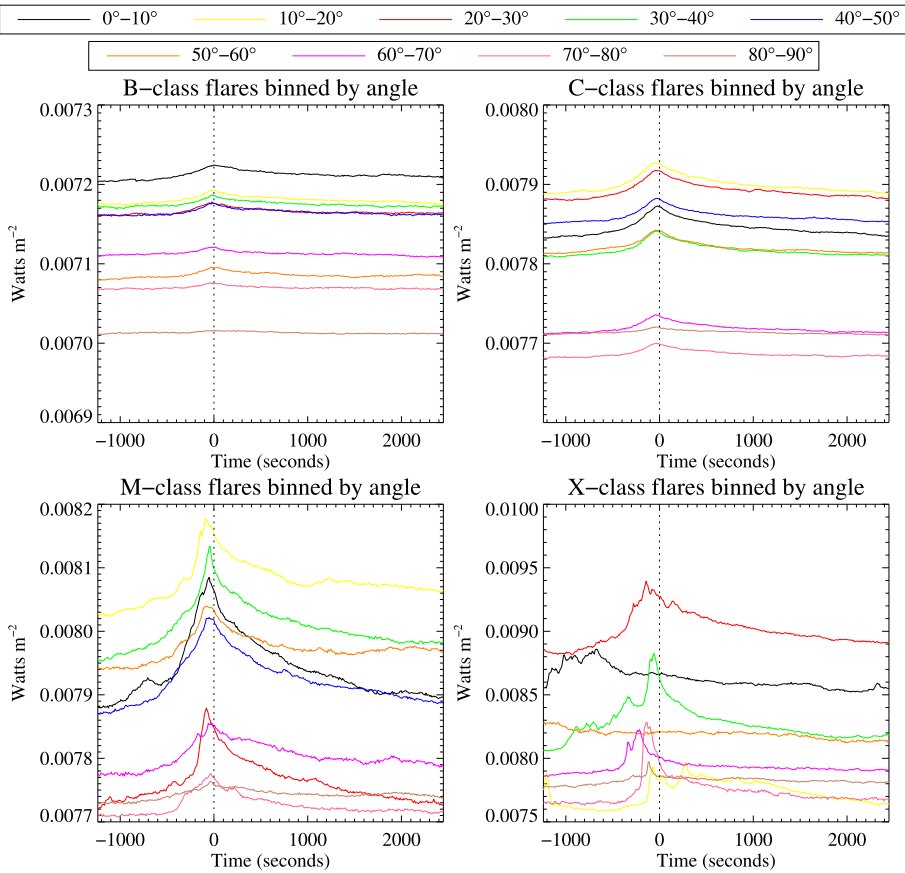
Figure 5 Plot of the Lyα time profiles for flares binned by heliographic angle in increments of 10 degrees for B-, C-, M-, and X-class flares. The vertical dashed line in each panel marks the time of the SXR peaks of all flares.

as derived by Brekke and Kjeldseth-Moe (1994) and also employed by Woods, Kopp, and Chamberlin (2006) and Milligan et al. (2020). R is the intensity at a given angle, R_C is the intensity ratio at disc center, k is the limb variation relative to center, and $\mu = \cos(\theta)$. The values of R_C for B-, C-, and M-class flares are 1.002, 1.004, and 1.021, respectively, while the corresponding k values are 0.99, 0.99, and 0.97. In agreement with Milligan et al. (2020), all flare classifications showed a smaller relative enhancement in Lyα emission for flares that occurred closer to the solar limb compared to those that occurred closer to disc center. While it would be more physically meaningful to normalize each curve to their respective GOES class (Woods, Kopp, and Chamberlin, 2006), the summed nature of the superposed-epoch analysis coupled with the difficulty associated with subtracting the solar background for smaller X-ray events, make this much more of a challenge, and is likely to return similar trends, albeit with much lower k-values. Note that Kretzschmar et al. (2010) and Kretzschmar (2011) did not include flares that occurred beyond 60° of disc center in their superposed-epoch analysis on flares in the TSI, visible, EUV, and SXR emission as they assumed that limb flares would not produce a measurable response at these wavelengths in the chromosphere.

Figure 6 Plot of the Lyα
contrast for each of the averaged
lightcurves in Figure 5
(excluding X-class flares) as a
function of heliographic angle.
The curves fitted to each GOES
class are given by Equation 1.
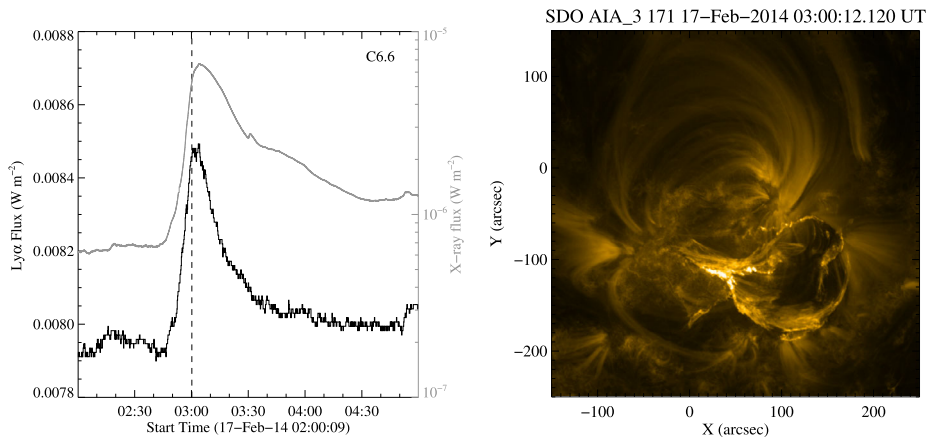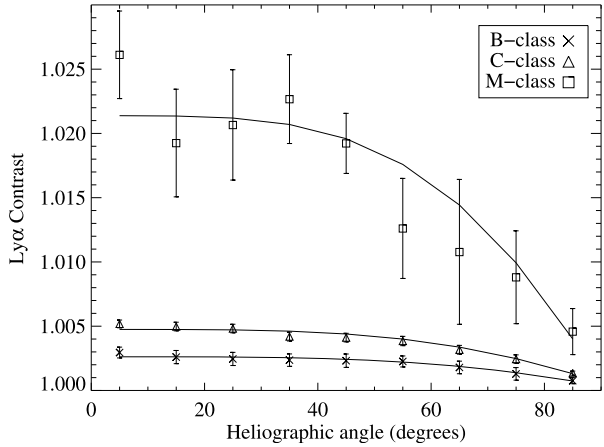
Figure 7 Left: Plot of Lyα (black) and X-ray (gray) time profiles for a C6.6 flare that occurred on 17 February 2014. The vertical dashed line denotes the time of the SDO/AIA image in the right hand panel. Right: SDO/AIA 171 Å image taken around the time of peak Lyα emission showing the possible failed filament eruption that may be responsible for the unusually high Lyα flux.

3.2. An Unusual C-class Flare

While the vast majority of B- and C-class flares do not produce a Lyα signature above the bright solar background, one event in this study—a C6.6 flare that occurred on 17 February 2014 (SOL2014-02-17)—displayed a remarkable 7% enhancement. Such a degree of contrast has hitherto only been associated with a few X-class flares (Woods et al., 2004; Milligan et al., 2020). Converting the flare excess in Lyα into units of energy for this event yielded a value of $\approx 10^{30}$ erg, which is comparable to that calculated for the 15 February 2011 X2.2 by Milligan et al. (2014) using Lyα data from the EUV Variability Experiment (EVE; Woods et al., 2012) on board the Solar Dynamics Observatory (SDO; Pesnell, Thompson, and Chamberlin, 2012). A plot of the Lyα and X-ray lightcurves for the event is shown in Figure 7, along with a 171 Å image from the Atmospheric Imaging Assembly (AIA; Lemen et al., 2012), also on SDO, taken around the time of peak emission (vertical dashed line

in left hand panel). Ordinarily, flare-related increases in Lyα (or indeed any inherent chromospheric emission) is primarily detected during the impulsive phase as the chromosphere is heated by precipitating particles from the corona, or late in the decay phase as hot flare plasma cools through instrumental passbands. Large increases in Lyα would therefore usually be attributed to a particularly energetic beam of electrons, and/or an unusually large footpoint area. Unfortunately, hard X-ray data from the Ramaty High Energy Solar Spectroscopic Imager (Lin et al., 2002) or Fermi (Meegan et al., 2009) were not available for this event, and so the parameters of the electron distribution that may have been responsible remains unknown. However, SDO/AIA data appear to show a failed filament eruption in all EUV channels (only 171 Å is shown in Figure 7). No associated coronal mass ejection could be seen in coronagraph images around the time and location of the flare. The Lyα emission from this event appears to correlate well with the main X-ray phase suggesting that the it could have been emanating from the corona as heating took place within the large volume of the filament. A similar conclusion was reached by Rubio da Costa et al. (2009) who reported co-spatial Lyα (from the Transition Region and Coronal Explorer; Handy et al., 1999) and X-ray emission during a filament eruption.

4. Conclusions

This article presents a study of 8579 solar flares observed in the Lyα line of neutral hydrogen. As weaker flares do not readily produce a Lyα signature above the intense solar background at this wavelength, a superposed-epoch analysis was carried out on 3123 B-class flares and 4972 C-class flares. On average, these flares were found to exhibit a $0.1 - 0.3\%$ enhancement. For completion and comparison, 453 M- and 31 X-flares were also coadded, and average increases of $1 - 4\%$ were measured. For each GOES classification, flares were also summed according to their heliographic location revealing that in all cases, flares closer to disc center displayed a greater enhancement on average than those that occurred closer to the solar limb due to the opacity of Lyα, or possible foreshortening of the flare ribbons. A C-class flare that exhibited an abnormally high contrast of 7% (equating to 10^{30} erg) was also presented.

While GOES/EUVS was designed as an EUV irradiance monitor, the results presented here show just how stable the data are and how they can be utilized for detailed scientific analysis, in particular for large scale statistical studies. Although the sensitivity of GOES-15/EUVS-E might be limited to larger flares, the new Lyα irradiance instruments that are part of the Extreme Ultraviolet and X-ray Irradiance Sensor (EXIS; Eparvier et al., 2009; Chamberlin et al., 2009) suite on the newly launched GOES-R series of spacecraft (GOES-16 and GOES-17 were launched in February 2017 and June 2018, respectively, with GOES-18 and GOES-19 to follow) will have a greater dynamic range, as well as will provide pseudo line profiles by sampling the Lyα profile in five wavelength pixels rather than as broadband measurements. Similarly, the imaging capability of the EUV Imager (EUI; Schühle et al., 2011; Rochus et al., 2020) on board Solar Orbiter will be able to spatially resolve flares in Lyα for the first time. The findings presented illustrate that even minor flares can produce small, but perceptible changes in the solar Lyα irradiance, and should therefore serve as a baseline for the advent of new Lyα flare observations and advanced numerical simulations that will become available during Solar Cycle 25.

are freely and publicly available from the instrument websites (GOES/EUVS: https://satdat.ngdc.noaa.gov/sem/goes/data/euvs/GOES_v4/G15/; GOES/XRS: https://www.ngdc.noaa.gov/stp/satellite/goes/dataaccess.html).

References

Baliukin, I.I., Bertaux, J.-L., Quémerais, E., Izmodenov, V.V., Schmidt, W.: 2019, SWAN/SOHO Lyman-α mapping: the hydrogen geocorona extends well beyond the Moon. *J. Geophys. Res. Space Phys.* **124**, 861. DOI. ADS.

Brekke, P., Kjeldseth-Moe, O.: 1994, The solar UV continuum 1440-1680 Å and its center-to-limb variation. *Solar Phys.* **150**, 19. DOI. ADS.

Brekke, P., Rottman, G.J., Fontenla, J., Judge, P.G.: 1996, The ultraviolet spectrum of a 3B class flare observed with SOLSTICE. *Astrophys. J.* **468**, 418. DOI. ADS.

Canfield, R.C., van Hoosier, M.E.: 1980, Observed L-alpha profiles for two solar flares - 14:12 UT 15 June, 1973 and 23:16 UT 21 January, 1974. *Solar Phys.* **67**, 339. DOI. ADS.

Chamberlin, P.C., Woods, T.N., Eparvier, F.G., Jones, A.R.: 2009, *Next Generation X-Ray Sensor (XRS) for the NOAA GOES-R Satellite Series*, SPIE Conf. Ser. **7438**, 743802. DOI. ADS.

Chubb, T.A., Friedman, H., Kreplin, R.W., Kupperian, J.E Jr.: 1957, Lyman alpha and X-ray emissions during a small solar flare. *J. Geophys. Res.* **62**, 389. DOI. ADS.

Dominique, M., Zhukov, A.N., Heinzel, P., Dammasch, I.E., Wauters, L., Dolla, L., Shestov, S., Kretzschmar, M., Machol, J., Lapenta, G., Schmutz, W.: 2018, First detection of solar flare emission in mid-ultraviolet Blamer continuum. *Astrophys. J. Lett.* **867**, L24. DOI. ADS.

Eparvier, F.G., Crotser, D., Jones, A.R., McClintock, W.E., Snow, M., Woods, T.N.: 2009, *The Extreme Ultraviolet Sensor (EUVS) for GOES-R*, SPIE Conf. Ser. **7438**, 743804. DOI. ADS.

Eparvier, F.G., Chamberlin, P.C., Woods, T.N., Thiemann, E.M.B.: 2015, The solar extreme ultraviolet monitor for MAVEN. *Space Sci. Rev.* **195**, 293. DOI. ADS.

Handy, B.N., Acton, L.W., Kankelborg, C.C., Wolfson, C.J., Akin, D.J., Bruner, M.E., Caravalho, R., Catura, R.C., Chevalier, R., Duncan, D.W., Edwards, C.G., Feinstein, C.N., Freeland, S.L., Friedlaender, F.M., Hoffmann, C.H., Hurlburt, N.E., Jurcevich, B.K., Katz, N.L., Kelly, G.A., Lemen, J.R., Levay, M., Lindgren, R.W., Mathur, D.P., Meyer, S.B., Morrison, S.J., Morrison, M.D., Nightingale, R.W., Pope, T.P., Rehse, R.A., Schrijver, C.J., Shine, R.A., Shing, L., Strong, K.T., Tarbell, T.D., Title, A.M., Torgerson, D.D., Golub, L., Bookbinder, J.A., Caldwell, D., Cheimets, P.N., Davis, W.N., Deluca, E.E., McMullen, R.A., Warren, H.P., Amato, D., Fisher, R., Maldonado, H., Parkinson, C.: 1999, The transition region and coronal explorer. *Solar Phys.* **187**, 229. DOI. ADS.

Hanser, F.A., Sellers, F.B.: 1996, Design and calibration of the GOES-8 solar x-ray sensor: the XRS. In: Washwell, E.R. (ed.) *GOES-8 and Beyond*, Proc. SPIE **2812**, 344. DOI. ADS.

Kretzschmar, M.: 2011, The Sun as a star: observations of white-light flares. *Astron. Astrophys.* **530**, A84. DOI. ADS.

Kretzschmar, M.: 2015, Temperature dependence of the flare fluence scaling exponent. *Solar Phys.* **290**, 3593. DOI. ADS.

Kretzschmar, M., Dominique, M., Dammasch, I.E.: 2013, Sun-as-a-star observation of flares in Lyman α by the PROBA2/LYRA radiometer. *Solar Phys.* **286**, 221. DOI. ADS.

Kretzschmar, M., de Wit, T.D., Schmutz, W., Mekaoui, S., Hochedez, J.-F., Dewitte, S.: 2010, The effect of flares on total solar irradiance. *Nat. Phys.* **6**, 690. DOI. ADS.

Lean, J.L.: 1985, Calculations of Lyman alpha absorption in the mesosphere. In: Zerefos, C.S., Ghazi, A. (eds.) *Atmospheric Ozone*, 697. Springer, Dordrecht. ADS.

Lemen, J.R., Title, A.M., Akin, D.J., Boerner, P.F., Chou, C., Drake, J.F., Duncan, D.W., Edwards, C.G., Friedlaender, F.M., Heyman, G.F., Hurlburt, N.E., Katz, N.L., Kushner, G.D., Levay, M., Lindgren, R.W., Mathur, D.P., McFeaters, E.L., Mitchell, S., Rehse, R.A., Schrijver, C.J., Springer, L.A., Stern, R.A., Tarbell, T.D., Wuelser, J.-P., Wolfson, C.J., Yanari, C., Bookbinder, J.A., Cheimets, P.N., Caldwell, D., Deluca, E.E., Gates, R., Golub, L., Park, S., Podgorski, W.A., Bush, R.I., Scherrer, P.H., Gummin, M.A., Smith, P., Auker, G., Jerram, P., Pool, P., Soufli, R., Windt, D.L., Beardsley, S., Clapp, M., Lang, J., Waltham, N.: 2012, The Atmospheric Imaging Assembly (AIA) on the Solar Dynamics Observatory (SDO). *Solar Phys.* **275**, 17. DOI. ADS.

Lin, R.P., Dennis, B.R., Hurford, G.J., Smith, D.M., Zehnder, A., Harvey, P.R., Curtis, D.W., Pankow, D., Turin, P., Bester, M., Csillaghy, A., Lewis, M., Madden, N., van Beek, H.F., Appleby, M., Raudorf, T., McTiernan, J., Ramaty, R., Schmahl, E., Schwartz, R., Krucker, S., Abiad, R., Quinn, T., Berg, P., Hashii, M., Sterling, R., Jackson, R., Pratt, R., Campbell, R.D., Malone, D., Landis, D., Barrington-Leigh, C.P., Slassi-Sennou, S., Cork, C., Clark, D., Amato, D., Orwig, L., Boyle, R., Banks, I.S., Shirey, K., Tolbert, A.K., Zarro, D., Snow, F., Thomsen, K., Henneck, R., McHedlishvili, A., Ming, P., Fivian, M., Jordan, J., Wanner, R., Crubb, J., Preble, J., Matranga, M., Benz, A., Hudson, H., Canfield, R.C., Holman, G.D., Crannell, C., Kosugi, T., Emslie, A.G., Vilmer, N., Brown, J.C., Johns-Krull, C., Aschwanden, M., Metcalf, T., Conway, A.: 2002, The Reuven Ramaty High-Energy Solar Spectroscopic Imager (RHESSI). *Solar Phys.* **210**, 3. DOI. ADS.

McClintock, W.E., Rottman, G.J., Woods, T.N.: 2005, Solar-stellar irradiance comparison experiment II (Solstice II): instrument concept and design. *Solar Phys.* **230**, 225. DOI. ADS.

Meegan, C., Lichti, G., Bhat, P.N., Bissaldi, E., Briggs, M.S., Connaughton, V., Diehl, R., Fishman, G., Greiner, J., Hoover, A.S., van der Horst, A.e.J., von Kienlin, A., Kippen, R.M., Kouveliotou, C., McBreen, S., Paciesas, W.S., Preece, R., Steinle, H., Wallace, M.S., Wilson, R.B., Wilson-Hodge, C.: 2009, The Fermi gamma-ray burst monitor. *Astrophys. J.* **702**, 791. DOI. ADS.

Meier, R.R., Prinz, D.K.: 1970, Absorption of the solar Lyman alpha line by geocoronal atomic hydrogen. *J. Geophys. Res.* **75**, 6969. DOI. ADS.

Milligan, R.O., Chamberlin, P.C.: 2016, Anomalous temporal behaviour of broadband Lyα observations during solar flares from SDO/EVE. *Astron. Astrophys.* **587**, A123. DOI. ADS.

Milligan, R.O., Ireland, J.: 2018, On the performance of multi-instrument solar flare observations during solar cycle 24. *Solar Phys.* **293**, 18. DOI. ADS.

Milligan, R.O., Kerr, G.S., Dennis, B.R., Hudson, H.S., Fletcher, L., Allred, J.C., Chamberlin, P.C., Ireland, J., Mathioudakis, M., Keenan, F.P.: 2014, The radiated energy budget of chromospheric plasma in a major solar flare deduced from multi-wavelength observations. *Astrophys. J.* **793**, 70. DOI. ADS.

Milligan, R.O., Fleck, B., Ireland, J., Fletcher, L., Dennis, B.R.: 2017, Detection of three-minute oscillations in full-disk Lyα emission during a solar flare. *Astrophys. J. Lett.* **848**, L8. DOI. ADS.

Milligan, R.O., Hudson, H.S., Chamberlin, P.C., Hannah, I.G., Hayes, L.A.: 2020, Lyman-alpha variability during solar flares over solar cycle 24 using GOES-15/EUVS-E. *Space Weather* **18**, e02331. DOI. ADS.

Neupert, W.M.: 1968, Comparison of solar X-ray line emission with microwave emission during flares. *Astrophys. J. Lett.* **153**, L59. DOI. ADS.

Pesnell, W.D., Thompson, B.J., Chamberlin, P.C.: 2012, The Solar Dynamics Observatory (SDO). *Solar Phys.* **275**, 3. DOI. ADS.

Raulin, J.-P., Trottet, G., Kretzschmar, M., Macotela, E.L., Pacini, A.r., Bertoni, F.C.P., Dammasch, I.E.: 2013, Response of the low ionosphere to X-ray and Lyman-α solar flare emissions. *J. Geophys. Res. Space Phys.* **118**, 570. DOI. ADS.

Rochus, P., Auchère, F., Berghmans, D., Harra, L., Schmutz, W., Schühle, U., Addison, P., Appourchaux, T., Aznar Cuadrado, R., Baker, D., Barbay, J., Bates, D., BenMoussa, A., Bergmann, M., Beurthe, C., Borgo, B., Bonte, K., Bouzit, M., Bradley, L., Büchel, V., Buchlin, E., Büchner, J., Cabé, F., Cadiergues, L., Chaigneau, M., Chares, B., Choque Cortez, C., Coker, P., Condamin, M., Coumar, S., Curdt, W., Cutler, J., Davies, D., Davison, G., Defise, J.-M., Del Zanna, G., Delmotte, F., Delouille, V., Dolla, L., Dumesnil, C., Dürig, F., Enge, R., François, S., Fourmond, J.-J., Gillis, J.-M., Giordanengo, B., Gissot, S., Green, L.M., Guerreiro, N., Guilbaud, A., Gyo, M., Haberreiter, M., Hafiz, A., Hailey, M., Halain, J.-P., Hansotte, J., Hecquet, C., Heerlein, K., Hellin, M.-L., Hemsley, S., Hermans, A., Hervier, V., Hochedez, J.-F., Houbrechts, Y., Ihsan, K., Jacques, L., Jérôme, A., Jones, J., Kahle, M., Kennedy, T., Klaproth, M., Kolleck, M., Koller, S., Kotsialos, E., Kraaikamp, E., Langer, P., Lawrenson, A., Le Clech', J.-C., Lenaerts, C., Liebecq, S., Linder, D., Long, D.M., Mampaey, B., Markiewicz-Innes, D., Marquet, B., Marsch, E., Matthews, S., Mazy, E., Mazzoli, A., Meining, S., Meltchakov, E., Mercier, R., Meyer, S., Monecke, M., Monfort, F., Morinaud, G., Moron, F., Mountney, L., Müller, R., Nicula, B., Parenti, S., Peter, H., Pfiffner, D., Philippon, A., Phillips, I., Plesseria, J.-Y., Pylyser, E., Rabecki, F., Ravet-Krill, M.-F., Rebellato, J., Renotte, E., Rodriguez, L., Roose, S., Rosin, J., Rossi, L., Roth, P.,

Rouesnel, F., Roulliay, M., Rousseau, A., Ruane, K., Scanlan, J., Schlatter, P., Seaton, D.B., Silliman, K., Smit, S., Smith, P.J., Solanki, S.K., Spescha, M., Spencer, A., Stegen, K., Stockman, Y., Szwec, N., Tamiatto, C., Tandy, J., Teriaca, L., Theobald, C., Tychon, I., van Driel-Gesztelyi, L., Verbeeck, C., Vial, J.-C., Werner, S., West, M.J., Westwood, D., Wiegelmann, T., Willis, G., Winter, B., Zerr, A., Zhang, X., Zhukov, A.N.: 2020, The Solar Orbiter EUI instrument: the extreme ultraviolet imager. *Astron. Astrophys.* **642**, A8. DOI. ADS.

Rubio da Costa, F., Fletcher, L., Labrosse, N., Zuccarello, F.: 2009, Observations of a solar flare and filament eruption in Lyman α and X-rays. *Astron. Astrophys.* **507**, 1005. DOI. ADS.

Schühle, U., Halain, J.-P., Meining, S., Teriaca, L.: 2011, The Lyman-alpha telescope of the extreme ultraviolet imager on Solar Orbiter. In: Fineschi, S., Fennelly, J. (eds.) *Solar Phys. and Space Weather Instrumentation IV*, *SPIE Conf. Ser.* **8148**, 81480K. DOI. ADS.

Viereck, R., Hanser, F., Wise, J., Guha, S., Jones, A., McMullin, D., Plunket, S., Strickland, D., Evans, S.: 2007, Solar extreme ultraviolet irradiance observations from GOES: design characteristics and initial performance. In: Fineschi, S., Viereck, R.A. (eds.) *Solar Phys. and Space Weather Instrumentation II*, *SPIE Conf. Ser.* **6689**, 66890K. DOI. ADS.

Woods, T.N., Kopp, G., Chamberlin, P.C.: 2006, Contributions of the solar ultraviolet irradiance to the total solar irradiance during large flares. *J. Geophys. Res. Space Phys.* **111**, A10S14. DOI. ADS.

Woods, T.N., Rottman, G.J., White, O.R., Fontenla, J., Avrett, E.H.: 1995, The solar LY alpha line profile. *Astrophys. J.* **442**, 898. DOI. ADS.

Woods, T.N., Tobiska, W.K., Rottman, G.J., Worden, J.R.: 2000, Improved solar Lyman α irradiance modeling from 1947 through 1999 based on UARS observations. *J. Geophys. Res.* **105**, 27195. DOI. ADS.

Woods, T.N., Eparvier, F.G., Fontenla, J., Harder, J., Kopp, G., McClintock, W.E., Rottman, G., Smiley, B., Snow, M.: 2004, Solar irradiance variability during the October 2003 solar storm period. *Geophys. Res. Lett.* **31**, L10802. DOI. ADS.

Woods, T.N., Chamberlin, P.C., Harder, J.W., Hock, R.A., Snow, M., Eparvier, F.G., Fontenla, J., McClintock, W.E., Richard, E.C.: 2009, Solar irradiance reference spectra (SIRS) for the 2008 whole heliosphere interval (WHI). *Geophys. Res. Lett.* **36**, L01101. DOI. ADS.

Woods, T.N., Eparvier, F.G., Hock, R., Jones, A.R., Woodraska, D., Judge, D., Didkovsky, L., Lean, J., Mariska, J., Warren, H., McMullin, D., Chamberlin, P., Berthiaume, G., Bailey, S., Fuller-Rowell, T., Sojka, J., Tobiska, W.K., Viereck, R.: 2012, Extreme Ultraviolet Variability Experiment (EVE) on the Solar Dynamics Observatory (SDO): overview of science objectives, instrument design, data products, and model developments. *Solar Phys.* **275**, 115. DOI. ADS.